Simulation of the Wicking Effect in a Two-Layer Soil Liner System

T-C. Jim Yeh, Amado Guzman, Rajesh Srivastava, Philip E. Gagnard and John H. Kramer

Waste Manag Res 1995 13: 363
DOI: 10.1177/0734242X9501300407

Waste Management & Research (1995) **13**, 363–378

SIMULATION OF THE WICKING EFFECT IN A TWO-LAYER SOIL LINER SYSTEM

T-C. Jim Yeh[1], Amado Guzman[1], Rajesh Srivastava[2], Philip E. Gagnard[3], and John H. Kramer[4]

[1]*Department of Hydrology and Water Resources, University of Arizona, Tucson, Arizona 85721, U.S.A.,* [2]*Department of Soil and Water Science, University of Arizona, Tucson, Arizona 85721, U.S.A.,* [3]*Rust Environment & Infrastructure, Inc., 6143 S. Willow Drive, Englewood, Colorado 80111, U.S.A., and* [4]*Vadose Zone Monitoring Laboratory, Institute for Crustal Studies, University of California, Santa Barbara, California, U.S.A.*

(*Received 11 May 1992, accepted in revised form 11 July 1994*)

A series of simulation runs were made using the computer model VSAFT2 (Yeh & Srivastava 1990) to estimate the "wicking" potential of five low-permeability liner materials including excel, celite slurry, kiln dust, rock creek clay and celite waste. The unsaturated hydraulic properties for these materials were assumed to be represented by the van Genuchten model (1978). The hypothetical liner system simulated consisted of 0.305 m (1 foot) of low permeability material underlain by a medium sand. The purpose of this modelling effort was to quantify the effects of liner thickness and leakage rate on the lateral spreading of the wetting front, and to determine the effectiveness of the diffusivity function in predicting the migration of the wetting front. Results indicate, as expected, that the liner material with the lowest permeability retards vertical movement the most; however, the horizontal wicking effect is also limited. Additional multi-layer liner systems will be simulated in the next phase of the project to improve liner wicking performance.

Key Words—Diffusivity, leakage rate, wicking effect, unsaturated flow, soil liner, landfill.

1. Introduction

Waste disposal facilities such as landfills, tailing ponds, and radioactive waste repositories in the U.S.A. commonly use liners to isolate industrial and municipal wastes from the accessible environment. Most of these liners are made of low permeability media such as clays and man-made materials. In some cases, the liner is made of a fine textured earth material overlying a coarse textured material.

It is a well-known fact that coarse material is more permeable than fine material under near saturated conditions. As the degree of saturation decreases (suction becomes more positive), the difference in conductivity between coarse and fine material, however, becomes smaller. Beyond a threshold suction value, coarse material can be less permeable than fine material. Therefore, under very dry conditions (beyond the threshold suction value), coarse textured material can act as a capillary barrier to water in fine textured material, until the moisture at the interface between the two materials builds up sufficiently to penetrate into the coarse material (Hillel 1971).

Due to the capillary barrier effect, leachate penetrating the fine and less permeable material in a liner system tends to spread out laterally in the fine material after the

0734–242X/95/040363+16 $12.00/0

wetting front advances to the interface between the fine and coarse material. This lateral migration along the interface is called the "wicking effect". Indeed, past studies have substantiated that both effects, the capillary barrier and the wicking, occur in a liner system consisting of a layer of fine textured material overlying a layer of coarse textured material (Frind *et al.* 1977, Johnson *et al.* 1983, McWhorter *et al.* 1983, Yeh *et al.* 1985).

The state of California requires detection of waste constituents escaping from waste disposal facilities before they reach ground water (California Administrative Code). Thus, the liner system consisting of a fine over a coarse material is highly desirable because of the capillary barrier and the wicking effect. These effects may enhance the lateral movement of water and solutes in such a manner that facilitates collection and monitoring of leachates from the waste disposal facilities, using a relatively sparse sampling network.

The effect of the capillary barrier and the wicking layer depends on the unsaturated properties of the coarse and fine material. This study investigates the wicking effect in two-layer liner systems using numerical experiments. It is expected that the outcome of this study will help ongoing field-scale experiments designed to observe and quantify the wicking effect.

In a previous study (Yeh *et al.* 1991), numerical simulation of the wicking effect within a two-layer liner consisting of chino clay and plainfield sand was conducted to investigate the effect of finite element size on the simulation results. It was found that coarseness of the grid or the presence of an impermeable vertical boundary near the source did not strongly affect the movement of moisture in the cases examined. The lack of lateral movement in the top layer (chino clay) was thought to be a consequence of the small lateral capillary gradient due to relatively wet initial conditions.

In this study, additional simulations were performed to quantify the wicking abilities of five low permeability materials. More specifically, the purpose of this modelling effort was: (i) to quantify the effect of the thickness of the low conductivity layer on the lateral spreading of the wetting front; (ii) to evaluate the effect of leakage rate on the lateral spreading; and (iii) to explore the possibility of defining a criterion by which the material that produces maximum wicking, and minimizes the water movement through the liner, could be selected.

2. Description of the physical setting

Flow through several hypothetical two-layer liners consisting of a low permeability clay-like material overlying a high permeability material was investigated. The liners were assumed to be slightly slanted with a slope of 3%. Vertical cross-sections with dimensions of 3.05 m (10 feet) in the horizontal and 0.915 m (3 feet) in the vertical, as depicted in Fig. 1, were used for most of the simulations. The thickness of the top, low conductivity layer was assumed to be 0.305 m (1 foot) and that of the bottom, high conductivity layer was 0.61 m (2 feet). The vertical dimension of the cross-section was varied in some simulations to study the effect of thickness on lateral spreading of the wetting front.

3. Material properties

Five materials, excel, celite slurry, kiln dust, rock creek clay and celite waste, with saturated hydraulic conductivity ranging from 1.8×10^{-6} to 7.3×10^{-4} mh^{-1}, were

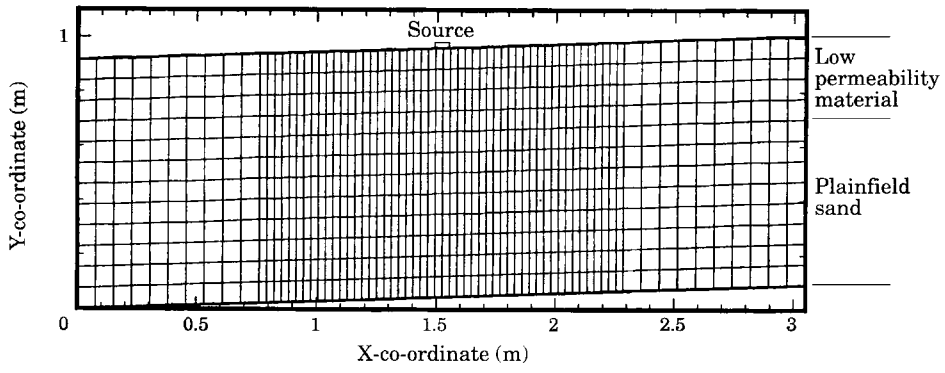

Fig. 1. Schematic representation of the simulated cross-section.

selected as candidates for the low permeability layer of the liner system. Plainfield sand was used as the coarse material for the bottom layer of the system. The unsaturated hydraulic properties of all these materials were assumed to be represented by the van Genuchten model (1978). That is, the moisture content–suction relationship (water release curve) of the materials is given by:

$$\theta(\psi) = (\theta_s - \theta_r)[1 + (\alpha\psi)^n]^{-m} + \theta_r \quad [1]$$

and the hydraulic conductivity–suction relationship is described by:

$$K(\psi) = K_s \frac{(1 - (\alpha\psi)^{n-1}[1 + (\alpha\psi)^n]^{-m})^2}{[1 + (\alpha\psi)^n]^{m/2}} \quad [2]$$

where K_s is the saturated hydraulic conductivity, and ψ is the suction. θ_s and θ_r are moisture content at saturation, and residual moisture content, respectively. α and n are parameters controlling the curvature of the relationships and $m = 1 - 1/n$.

By adopting this model, it is assumed that the relationship between the unsaturated hydraulic conductivity and suction for the materials can be obtained by knowing the moisture content–suction relationship and the saturated hydraulic conductivity values. Laboratory determinations of the water release curves and the saturated hydraulic conductivity values for the five materials were conducted at the University of California at Santa Barbara, U.S.A. Equation 1 was then fitted to the measured water content and suction data by using a non-linear least square model (van Genuchten 1978) to obtain the parameters of the model; α, n, and θ_r. The plots of the data and water release curves estimated by the non-linear least square procedure are included as Appendix 1. The water content and suction data for the plainfield sand was obtained from a soil catalogue (Mualem 1976) and fitted in the same fashion as described above. Table 1 summarizes the model parameters for the six materials used in the simulations. Using these parameter values, hydraulic conductivity and suction curves for the six materials were generated by Equation 2. Graphical representation of the volumetric water content and the hydraulic conductivity as a function of suction for these materials are presented as Figs 2 & 3, respectively.

TABLE 1
Hydraulic properties for the layers

Layer	K_s (mh^{-1})	θ_s	θ_r	α (m^{-1})	n
Excel	7.3×10^{-4}	0.95	0.413	1.093	1.832
Celite slurry	1.5×10^{-4}	0.84	0.499	0.397	1.814
Kiln dust	7.3×10^{-5}	0.72	0.192	1.070	2.305
Rock creek clay	1.8×10^{-6}	0.395	0.325	1.070	2.425
Celite waste	3.7×10^{-5}	0.98	0.640	0.512	3.130
Plainfield sand	1.08	0.36	0.030	2.405	15.04

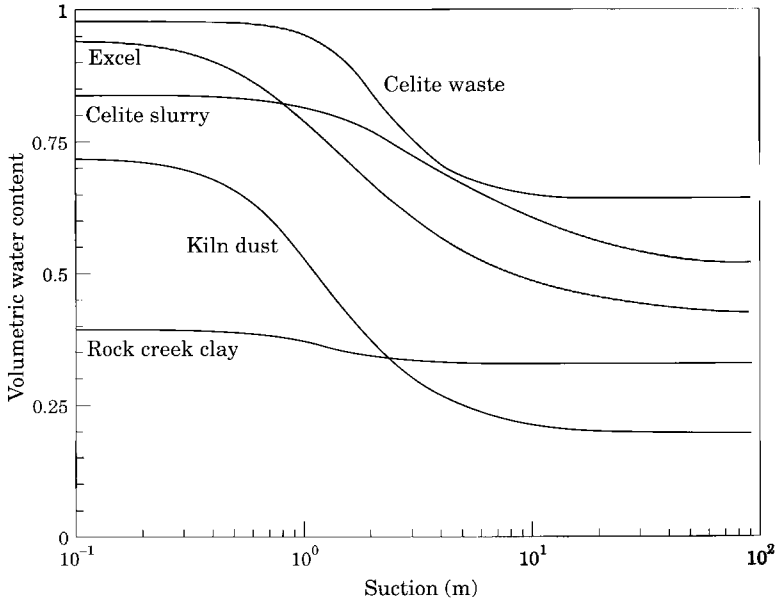

Fig. 2. Moisture release curves for the low conductivity materials.

4. Initial and boundary conditions

Initial conditions for all the simulations in this study were assigned to represent a state of hydrostatic equilibrium with a uniform total head distribution of −9.14 m (−30 feet) everywhere in the vertical cross-section. This initial condition implies that there was no moisture movement in the liner before the occurrence of the leakage. The corresponding suction pressure varied from −9.14 m in the bottom left corner to −10.15 m (−33.3 feet) at the top right corner of the cross-section. The volumetric water contents of the layers for this initial suction distribution can be obtained using the water release curves presented in Fig. 2.

Boundary conditions of the liner system were assigned as follows: no flow along the

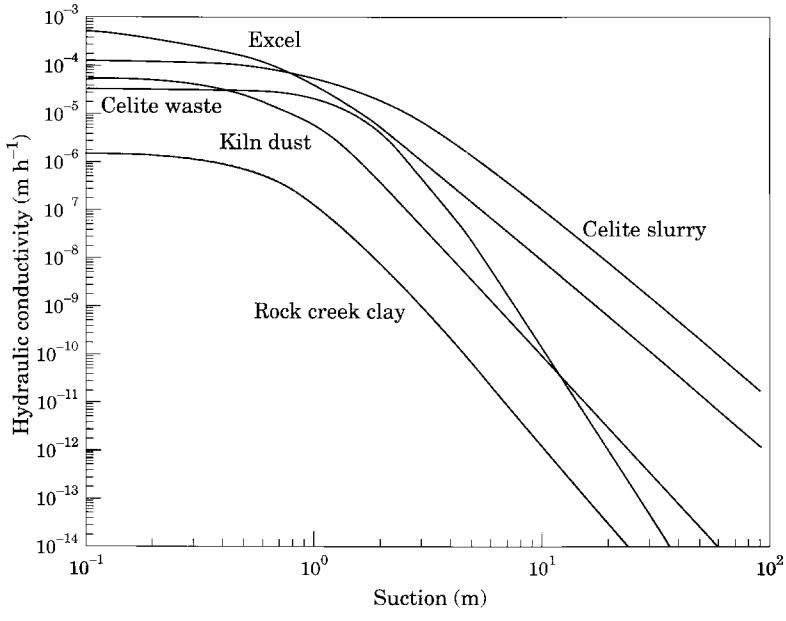

Fig. 3. Hydraulic conductivity curves for the low permeability materials.

top, left and right boundaries of the cross-section, and unit gradient conditions along the lower boundary. Point source leakage from the landfill to the liner was treated as a constant flow-rate at the three centre nodes along the top boundary. Several different flow-rates were used to examine their effects on the performance of the liner. The unit gradient condition at the bottom of the cross-section was used to circumvent the problem with the unknown boundary condition at this location. Otherwise, the fluid behaviour at the interface may be affected by other conditions specified at this boundary. Employing the unit gradient boundary condition at the bottom of the coarse layer is tantamount to considering the coarse layer to be of infinite vertical extent.

5. Numerical model

The numerical experiments are based on the numerical solution of the Richards equation for unsaturated flow:

$$\nabla \cdot [K(\psi)\, \nabla \cdot (\psi + z)] = C(\psi) \frac{\partial \psi}{\partial t} \qquad [3]$$

where, $K(\psi)$ is the hydraulic conductivity, $C(\psi)$ is the specific moisture capacity which indicates the change in moisture content due to a unit change in suction ψ, z is the vertical co-ordinate (positive downward), and t is the time. Equation 3 is non-linear in that the parameters K and C are strongly dependent on the suction, ψ. The computer model, VSAFT2, (Yeh & Srivastava 1990) was used to obtain the numerical solution of the above equation. This model is based on the Galerkin finite element technique and utilizes both the Picard and Newton approach for the non-linear iterations. The

code has been tested under various flow and transport situations, and has been found to be quite robust and accurate, mass balance errors being typically less than 5%.

6. Results

Results of the numerical experiments, simulating the performance of the liners under various leakage conditions, are analysed and discussed in the following sections. Effect of materials, thickness of the low permeability layer, and leakage rate on the lateral spreading along the interface are examined.

6.1 Effect of thickness on lateral spreading

The thickness of the low permeability layer is one of the important factors to be considered in the design of a liner system because it affects the arrival time of the leachate from the top of the liner to the interface, and the degree of lateral migration of the leachate within the fine material. A desirable liner should maximize the arrival time and the degree of lateral spreading, so that it can retard leachate migration and allow for a relatively sparse monitoring network.

Intuitively, as the thickness of the fine textured layer is increased, the time for the front to reach the interface will increase. In turn, the lateral spreading of the front should increase as a result of the larger residence time. In order to quantify the relationship between thickness and lateral spreading, four simulations with different thickness for the low permeability layer (kiln dust) were carried out. The thickness was varied from 0.15 to 1.22 m (0.5–4.0 feet). Spatial discretization of the liner for the first three thicknesses consisted of 923 nodes and 840 finite elements (Fig. 1). The finite element grid for the simulation of the 1.22 m thick, low conductivity layer consisted of 1492 nodes and 1400 elements. The vertical and horizontal distances between adjacent nodes were kept constant for these simulations, regardless of number of nodes and elements. The flux at the three central nodes was set equal to the saturated hydraulic conductivity of the kiln dust (Table 1) for all four simulations. Each simulation was extended until the time at which the leachate front barely touched the interface. The leachate front (wetting front) was defined as the front where the moisture content increased by 10% from the initial condition. Had a different definition of the wetting front been used, the absolute values for wetting front movement and time to reach the interface would have been different. However, the ratio of horizontal to vertical movement would still remain the same.

The ability of a given layer to retard vertical movement is directly related to the time it takes for the wetting front to reach the interface. Figure 4 presents the time to reach the interface as a function of the thickness, and shows that the time is related to the thickness in a quadratic fashion.

The relationship between lateral spreading along the top boundary (measured from a line bisecting the constant flux source) and the vertical movement is depicted in Fig. 5, which indicates that for kiln dust, lateral spreading is about 80% of the vertical movement (thickness) along the low permeability layer by the time that the wetting front reaches the interface. The difference between horizontal and vertical movement is due to gravity. For the other materials, it is expected that the relationship between vertical and horizontal movement will also be linear, although the proportionality constant may be different. This relationship helps to determine how much spreading will occur before the wetting front completely penetrates the low conductivity layer.

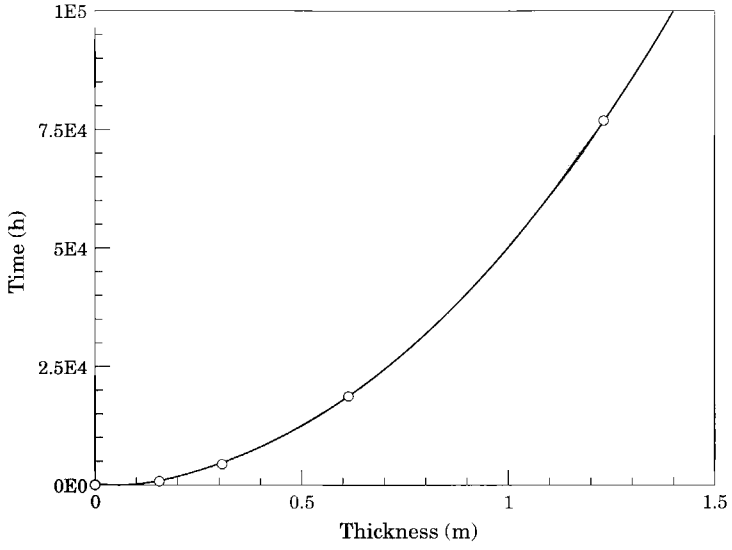

Fig. 4. Effect of thickness on the time to reach the interface.

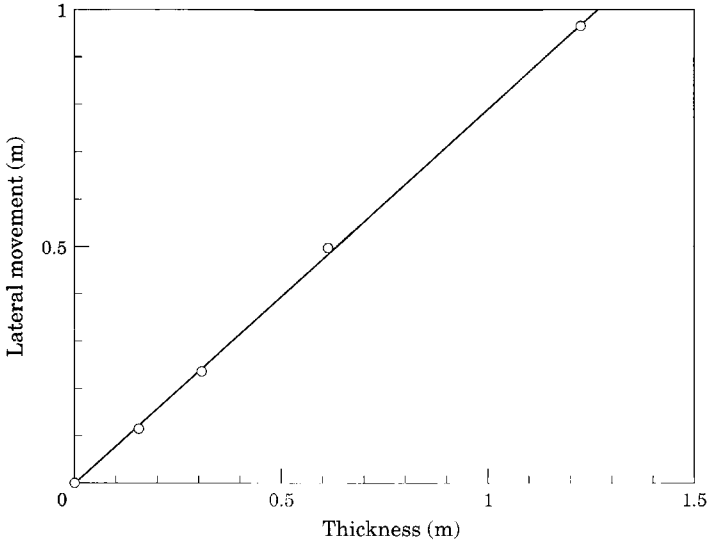

Fig. 5. Lateral spreading along the top boundary as a function of thickness.

The results of these four simulations indicate that, doubling the thickness of the low permeability layer will double the lateral spreading along the top. However, the time to reach the interface will be at least four times as large. These results imply, for monitoring purposes, that a thick layer may allow larger distances between monitoring locations. However, for the subsequent field-scale experiments, the time to collect a sample from these locations may be impractical. In actual liner systems, the thickness should be as large as possible and only limited by engineering and economic constraints.

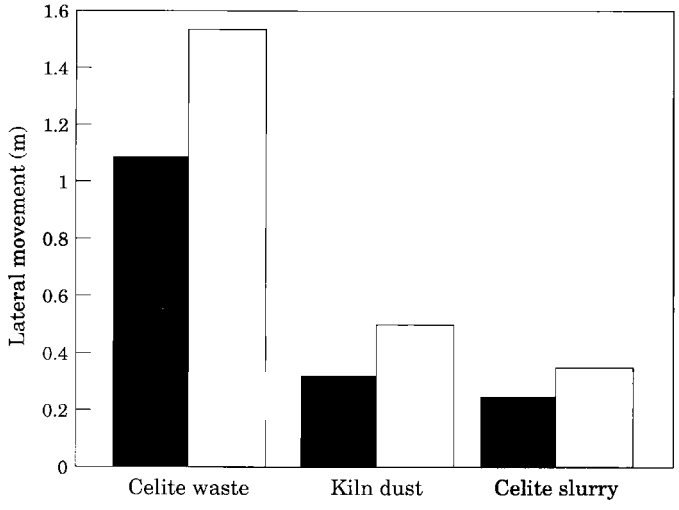

Fig. 6. Effect of the flow rate on the lateral migration. Solid bar, $q = K_s$; open bar, $q = 0.2\ K_s$.

6.2 *Effect of leakage rate on wicking*

Two sets of simulations were carried out with three different materials to quantify the effects of leakage rate on the lateral spreading of the wetting front. In the first set of simulations, the rate through the top boundary was set equal to the magnitude of the saturated hydraulic conductivity of each material, and in the other set was equal to 20% of the saturated conductivity. The total infiltration volume for both sets of simulations was kept constant by running the second set of simulations five times longer than the first set. This constant infiltration volume allows comparison of the degree of the migration at the end of the simulations. Obviously, if the same simulation time were used, the set with a larger flow-rate would show greater lateral spreading, thereby making the comparison meaningless. The degree of lateral migration as a function of leakage rate for the three different materials is illustrated in Fig. 6. Evidently, for the same total infiltration volume, a small flow-rate produces larger lateral spreading than a larger flow-rate. This is attributed to the fact that the time required to infiltrate the same volume is longer with a small leakage rate. Consequently, the opportunity for water to imbibe into a given material is enhanced.

To quantify the wicking ability of the five low conductivity materials, their diffusivities (D) were computed as follows:

$$D(\psi) = \frac{K(\psi)}{C(\psi)} \qquad [4]$$

Figure 7 depicts the diffusivities as a function of suction for the five materials. Based on this figure, one may conclude that lateral spreading in celite slurry should be larger than that in rock creek clay. The spreading in celite waste, however, will be larger, or smaller, than that in the other four porous materials depending on the range of suction. For example, for suction values smaller than 0.3 m (1 foot), the spread in celite waste will be larger than that in any of the remaining four materials. Nonetheless, as the suction increases, say from 0.3 to 3.05 m (1 to 10 feet), spread in celite waste may be

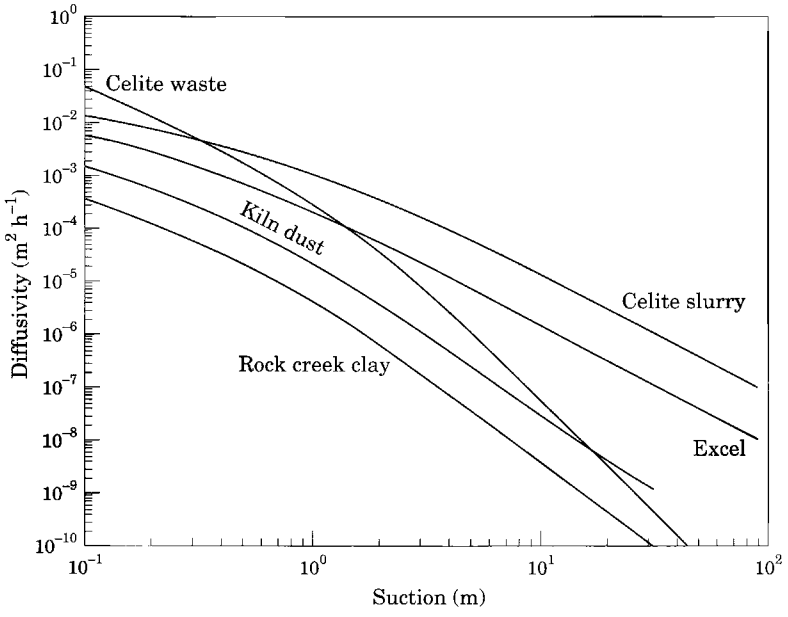

Fig. 7. Diffusivity functions for the low-permeability materials.

less than that in celite slurry, and as the suction approaches 3.05 m (10 feet) it may become less than that in excel.

Three additional simulations were conducted varying the material in the low conductivity layer to verify the ability of the diffusivity function to predict the migration of the wetting front. The materials used in these simulations were: kiln dust, excel and celite slurry. The finite element grid was kept the same (923 nodes and 840 elements) for these simulations. The leakage rate at the top boundary was set equal to the saturated hydraulic conductivity of the kiln dust (7.3×10^{-5} mh^{-1}). Using this leakage rate, the three materials remained under a state of partial saturation for the duration of the simulations.

The output of these simulations is analysed in terms of the square of the lateral spreading as a function of simulation time, in keeping with the diffusive nature of the spreading. The square of the lateral movement (L^2) along the interface vs. time after the wetting front has contacted the interface is presented in Fig. 8. This shows a clear linear relationship between L^2 and time after contact for the three different materials. From the abscissae of these lines, as indicated by the magnitude of the diffusivity (Fig. 7), celite slurry produces the maximum lateral spreading, followed by excel and then by kiln dust. Notice, however, that the maximum spreading (i.e. celite slurry) after 5000 h is only about 0.46 m (1.5 feet) and even at very large times (70,000 h), no break through into the lower layer was observed. The relationships between the diffusivity curves may explain why the spreading in excel is closer to that of celite slurry than to that of kiln dust. The difference between diffusivity values at a given suction is larger for kiln dust and excel than for celite slurry and excel.

The diffusivity function indicates that the material which maximizes the wicking effect, under suction values representative of field conditions, is celite slurry. However, the material which minimizes the vertical movement for the given leakage rate is kiln

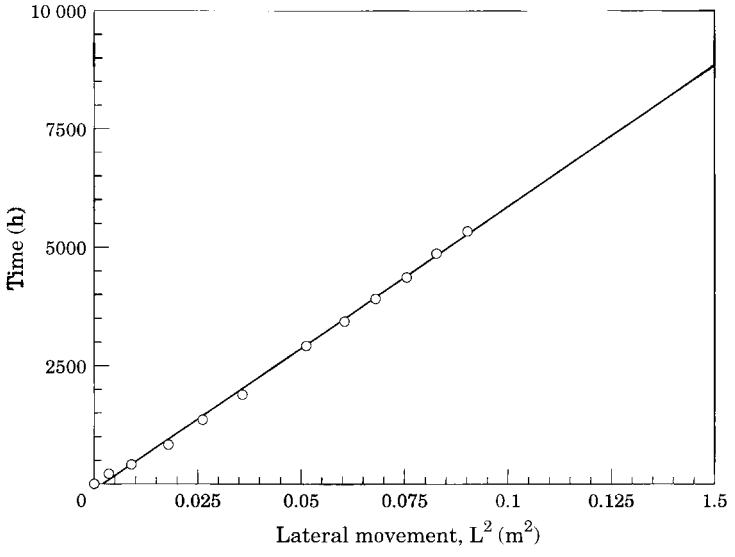

Fig. 8. Lateral movement along the interface as a function of time after contact.

TABLE 2
Time to reach the interface with leakage rate equal to the saturated hydraulic conductivity of the kiln dust

Material	Time (h)
Excel	2,750
Celite slurry	5,250
Kiln dust	19,100

dust (Table 2). This suggests that, if one desires to minimize the vertical movement of infiltrating water, the material with the minimum permeability should be selected (Table 1). It can be concluded that maximizing the wicking effect of a layer may result in unacceptable large vertical movement.

6.3 Wicking ability of the five candidate materials

The quadratic relationship between layer thickness and time to reach the interface (Fig. 4), and the linear relationship between lateral spreading and the vertical movement (Fig. 5) suggest that if lateral spreading (L) is plotted as L^2 vs. time, a linear relationship should be obtained. This behaviour, as expected based on the nature of Equation 3, is typical of a diffusion controlled process. That the spreading of the leachate front is governed by a diffusion-like process is easy to visualize for times prior to the front contacting the interface. After the contact, the same may not be true and the movement along the interface may or may not exhibit this behaviour. In order to further verify this behaviour, two plots were prepared: one showing the relation between the square

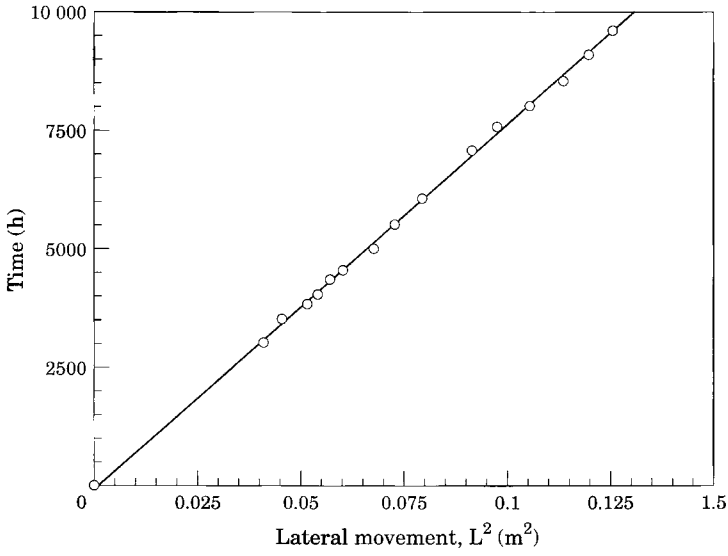

Fig. 9. Lateral movement along the top boundary as a function of time.

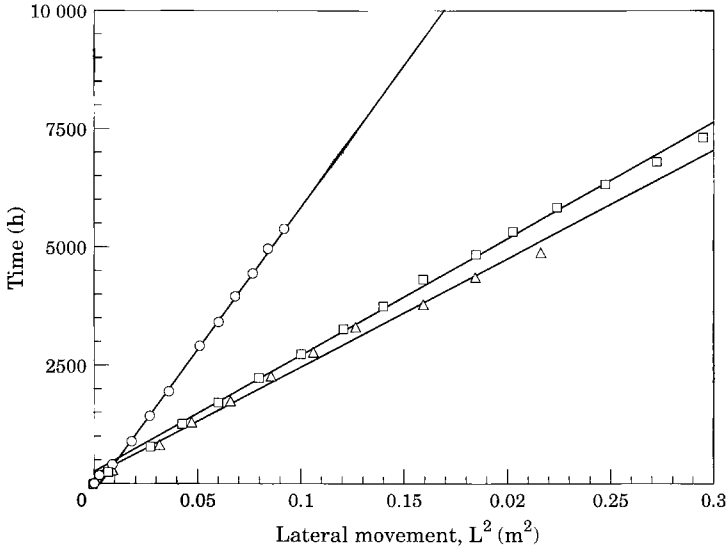

Fig. 10. Lateral movement of the wetting front as a function of time after contact. ○, Kiln dust; □, Excel; △, Celite slurry.

of lateral movement along the top boundary and the simulation time (Fig. 9), and the other showing the square of the lateral movement along the interface as a function of time after the wetting front has reached the interface (Fig. 10). From these figures, the square of the lateral movement along both boundaries, top and interface, is indeed linearly related to the time. These findings confirm that the lateral spreading is controlled by the diffusivity of the material. It will suffice to compute the diffusivities for each of

the five candidate materials, and then select the one with the maximum diffusivity within the suction range of interest.

7. Summary and conclusions

Performance of hypothetical two-layer liner systems was evaluated using numerical simulations. Five materials; excel, celite slurry, kiln dust, rock creek clay and celite waste, were selected as candidates for the low permeability layer of the liner system. Plainfield sand was used as the coarse material for the bottom layer of the system. Various simulations were conducted to investigate the effect of the thickness of the low conductivity layer on the lateral spreading of the wetting front, to evaluate the effect of leakage rate on the lateral spreading, and to define a criterion for selecting liner materials.

Results of the simulations indicated that the ratio of the vertical to horizontal movement of the wetting front before reaching the interface is constant with time. It was also found that doubling the thickness of the low permeability layer doubles the lateral spreading along the top layer, and that the time to reach the interface increases in a quadratic fashion as a function of the thickness. The quadratic relationship between the thickness and time to reach the interface illustrates the diffusive nature of the leakage movement within the low permeability layer. Therefore, it will suffice to use the diffusivities of the candidate materials as a criterion for selecting the one which may produce the maximum wicking effect. The results of several simulations verify this selection criterion.

For monitoring purposes, a thick layer may allow larger distances between sample ports because of larger lateral spreading resulting from longer residence times. However, for the ongoing field-scale experiments, the time to collect a sample from such ports may be impractical. In actual liners the thickness should be as large as possible and only limited by engineering and economic constraints.

Based on the diffusivity criterion, it is concluded that the material which maximizes the wicking effect, under suction values representative of field conditions, is celite slurry. However, the material which minimizes leachate vertical movement is rock creek clay, which has the smallest saturated hydraulic conductivity. Therefore, if minimizing the vertical movement of infiltrating water is the sole objective, rock creek clay should be selected. Apparently, maximizing the wicking effect and minimizing vertical movement through the low permeability layer are not compatible.

Results of the simulations also indicated that a small flow-rate produces larger lateral spreading than a larger rate for a given infiltration volume.

According to the results of the present study, it is evident that the lowest permeability material is most suitable for the top layer of a two-layer liner system because it can effectively retard vertical movement of any leachate. However, such a material does not produce a significant wicking effect and thus, may require a closely spaced monitoring network to satisfy requirements of regulatory agencies.

An additional concern associated with the two-layer liner is that in the presence of preferential flow paths in the low permeability layer, the retarding capacity of the clay may be diminished and flow through these paths may quickly overcome the capillary barrier presented by the bottom layer. Once the leachate penetrates the high conductivity layer in such a manner, it will move rapidly to the formations underlying the waste disposal facility without significant lateral spreading in the liner.

A safety liner may be constructed by using a three-layer system composed of a layer of fine sand-like material in between a top layer of a low conductivity, clay-like material and a bottom layer of a high conductivity material. Some apparent advantages of such a three-layer system over the two-layer system are: (i) monitoring, as required by regulatory entities, can be achieved with a relatively sparse sampling network along the intermediate sand-like layer and the time to collect a meaningful sample can be dramatically reduced; (ii) such a system also lessens the possibility of leachate penetrating the second interface as a result of capillary barrier effect of the coarse material below, and the wicking effect due to the large diffusivity of the fine sand-like material. Any leachate reaching this interface will quickly spread laterally in the middle layer due to its higher relative permeability, as compared to that of the clay layer; and (iii) any preferential flow (such as flow along cracks and fingers arising from instability), would be quickly diverted laterally as explained above and easily detected by the monitoring network.

The three-layer scheme is conceptually appealing as a better liner system for waste disposal facilities. To verify the suitability of this concept, quantify its advantages and establish criteria for selecting materials for the layers, further numerical simulations must be undertaken.

Acknowledgement

Funding for this study was provided by Waste Management of North America through its Research Office.

References

California Administrative Code, Title 23, Chapter 3, Subchapter 15, Article 15.

Frind, E. O., Gillham, R. W. & Pickens, J. F. (1977). *Application of Unsaturated Flow Properties in the Design of Geologic Environments for Radioactive Waste Storage Facilities.* Finite Elements in Water Resources. U.S.A.: Pentech Press.

Hillel, D. (1971). *Soil and Water: Physical Principles and Processes.* New York, U.S.A.: Academic Press.

Johnson, T. M., Cartwright, K., Herzog, B. L. & Larson, T. H. (1983). Modeling of Moisture Movement through Layered Trench Covers. In *Role of the Unsaturated Zone in Radioactive and Hazardous Waste Disposal* (J. W. Mercer, P. S. C. Rao & I. W. Marine, eds). Michigan, U.S.A.: Ann Arbor Science.

Mualem, Y. (1976). A Catalog of the Hydraulic Properties of Unsaturated Soils, Development of Methods, Tools and Solution for Unsaturated Flow with Application to Watershed Hydrology and Other Fields. *Research Project 442*, Technion Israel Institute of Technology, Haifa, Israel.

McWhorter, D. B., Nelson, J. D., Shepherd, T. A. & Wardwell, R. E. (1983). Role of Partially Saturated Soil in Liner Design for Hazardous Waste Disposal Sites. In *Role of the Unsaturated Zone in Radioactive and Hazardous Waste Disposal* (J. W. Mercer, P. S. C. Rao & I. W. Marine, eds). Michigan, U.S.A.: Ann Arbor Science.

van Genuchten, M. Th. (1978). Calculating the Unsaturated Hydraulic Conductivity with a New Closed-Form Analytical Model, *Research Report No. 78-WR-08*, Princeton University, New Jersey, U.S.A.

Yeh, T.-C., Gelhar, L. W. & Gutjahr, A. L. (1985). Stochastic analysis of unsaturated flow in heterogeneous soils. 3. Observations and applications. *Water Resources Research* **21**, pp. 465–471.

Yeh, T.-C. *et al.* (1991). *Numerical Simulation of the Wicking Effect*; a Progress Report Submitted to Waste Management of North America, Inc.

Yeh, T.-C. & Srivastava, R. (1990). VASFT2: Variably Saturated Flow and Transport in 2-Dimensions. A Finite Element Simulator. Department of Hydrology and Water Rscs. *Technical Report No. HWR 90-010*, University of Arizona, Tucson, U.S.A.

Appendix 1

Measured vs. fitted release curves

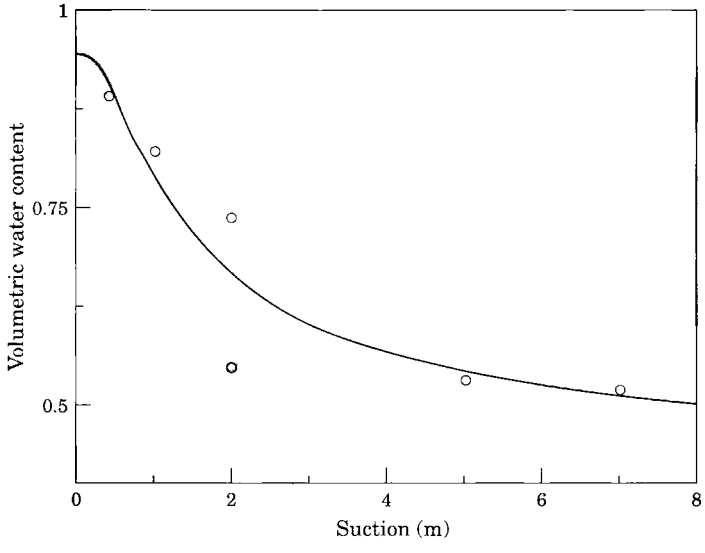

Fig. A1. Comparison of the van Genuchten model with experimental data: excel. ○, observed; —, model.

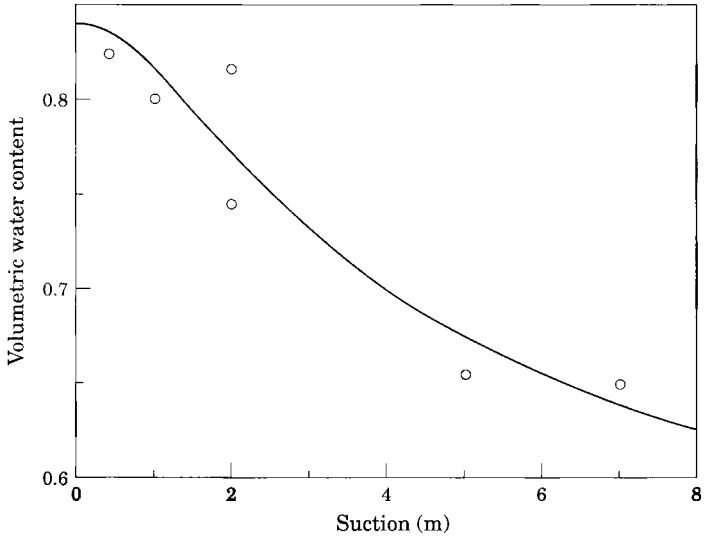

Fig. A2. Comparison of the van Genuchten model with experimental data: celite slurry. ○, observed; —, model.

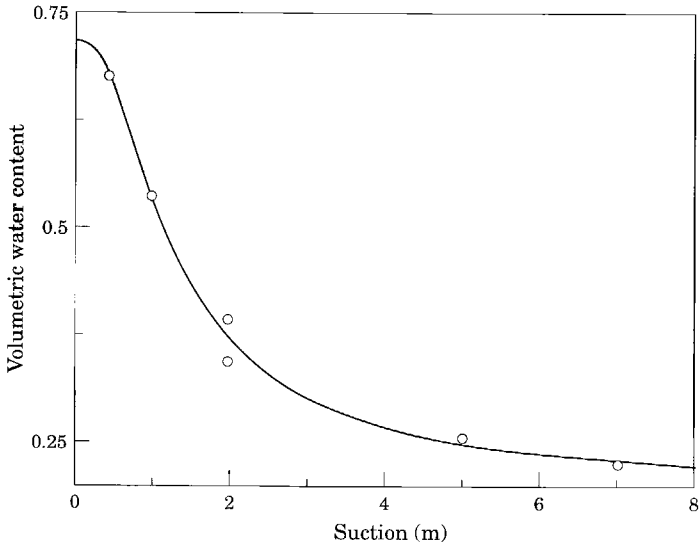

Fig. A3. Comparison of the van Genuchten model with experimental data: kiln dust. ○, observed; —, model.

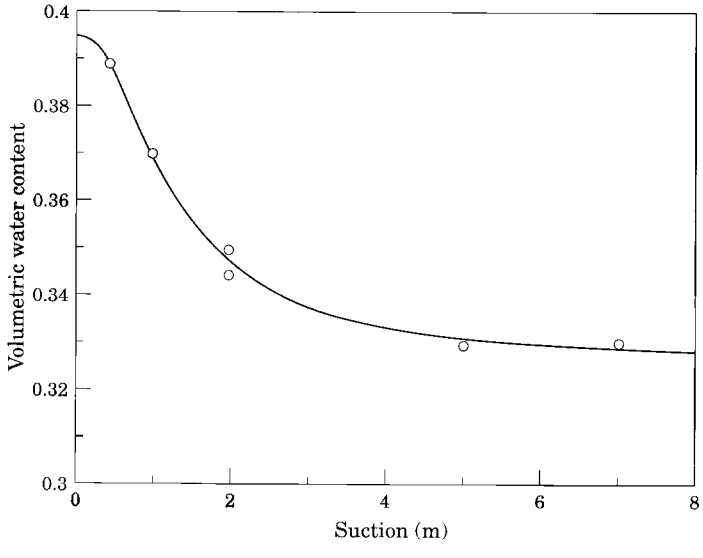

Fig. A4. Comparison of the van Genuchten model with experimental data: rock creek clay. ○, observed; —, model.

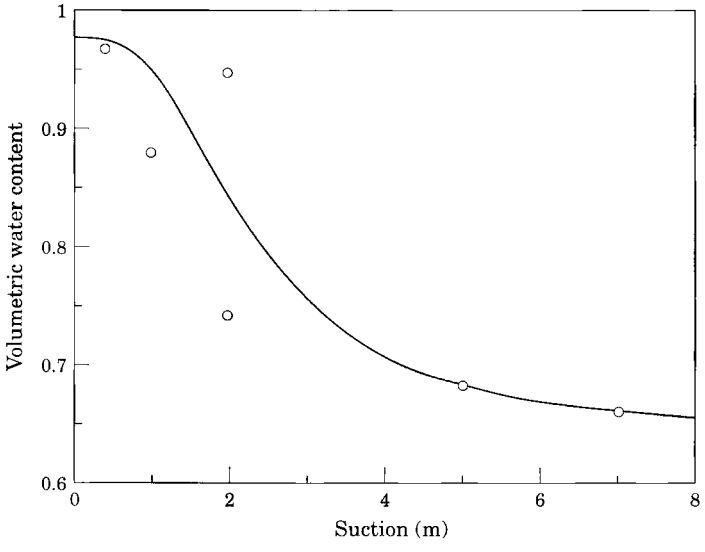

Fig. A5. Comparison of the van Genuchten model with experimental data: celite waste. ○, observed; —, model.